

ALPHA-DOT OR NOT: COMPARISON OF TWO SINGLE ATOM OPTICAL CLOCKS

T. ROSEN BAND*, D.B. HUME, C.-W. CHOU, J.C.J. KOELEMEN†, A. BRUSCH‡,
S. BICKMAN, W. H. OSKAY¶, T.M. FORTIER, J.E. STALNAKER§, S.A.
DIDDAMS, N.R. NEWBURY, W.C. SWANN, W.M. ITANO, D.J. WINELAND, AND
J.C. BERGQUIST

*National Institute of Standards and Technology,
325 Broadway, Boulder, CO 80305
E-mail: trosen@boulder.nist.gov

Repeated measurements of the frequency ratio of $^{199}\text{Hg}^+$ and $^{27}\text{Al}^+$ single-atom optical clocks over the course of a year yield a constraint on the possible present-era temporal variation of the fine-structure constant α . The time variation of the measured ratio corresponds to a time variation in the fine structure constant of $\dot{\alpha}/\alpha = (-1.6 \pm 2.3) \times 10^{-17}/\text{year}$, consistent with no change. The frequency ratio of these clocks was measured with a fractional uncertainty of 5.2×10^{-17} . Stability simulations for optical clocks whose probe period is limited by $1/f$ -noise in the laser local oscillator provide an estimate of the optimal probe period, as well as a modified expression for the theoretical clock stability.

1. Introduction

Recent analyses and modeling of astrophysical and geophysical data have produced conflicting reports of temporal and spatial variations of the fundamental “constants”. The conflicting evidence of change, and its important ramifications if true, has triggered a number of experimental efforts toward finding unambiguous evidence of such a variation.^{1,2} Much of the experimental work so far has been focused on a search for a variation of the fine structure constant α . The astrophysical and geophysical studies mentioned above attain high sensitivity to small temporal changes in α by observ-

†Present address: Dept. of Physics and Astronomy, Vrije Universiteit Amsterdam, The Netherlands

‡Present address: Niels Bohr Institute, University of Copenhagen, Denmark

¶Present address: Stanford Research Systems, Sunnyvale, CA

§Present address: Dept. of Physics and Astronomy, Oberlin College, Oberlin, OH

ing physical phenomena that occurred long ago and comparing these with the corresponding phenomena today. The prominent examples include the geochemical remains of the Oklo natural nuclear reactor³ and the astronomical observations of spectroscopic absorption lines from distant interstellar clouds with a quasar used as the light source.⁴ However, the analysis of data from Oklo, as well as that from distant quasars, is complicated by difficult quantitative interpretations that have produced discrepancies (see refs. 5 and 6 for example).

Since the energies of optical atomic transitions can be parameterized simply in terms of the fine structure constant α , two or more well stabilized and accurate optical clocks offer an alternate approach to the measurement of $d\alpha/dt$ - repetitive measurements of their frequency ratio(s) over time. At NIST, the Hg^+/Al^+ clock ratio measurements have now reached a precision sufficiently high that a year-long search for a linear time variation of α , or other fundamental constants, can be performed with a sensitivity higher than that offered by the geological and cosmological observations for the present era. High accuracy frequency comparison experiments between atomic clocks are also useful to search for violations of Local Position Invariance (LPI), which is a fundamental tenet of Einstein's Theory of General Relativity. A check for possible violations of LPI can be made by looking for correlations between the frequency ratio of two atomic clocks and the change of the gravitational potential due, for example, to the revolution of the Earth around the Sun.^{7,8}

We refer the reader elsewhere for a more comprehensive description of the Hg^+ and Al^+ single-ion, optical clocks (see, for example, refs. 9 and 10). Likewise, the significant contributions to the systematic frequency uncertainty of each optical clock have been described previously.^{11,12} Here we briefly summarize the dominant frequency uncertainties of each of the two clocks (Sec. 2 and 3) and then present a unitless measurement of their frequency ratio that spans a year. From the results of these highly accurate frequency ratio measurements, an estimate of the temporal stability of the constant α can be provided.

2. Summary of Hg^+ Clock Systematics

The residual motion of the laser-cooled Hg^+ ion gives rise to a fractional frequency uncertainty associated with the relativistic time dilation shift. The uncertainty due to the secular motion is constrained to be below 4×10^{-18} when the ion is cooled to near the Doppler cooling limit; the uncertainty due to residual micro-motion is also constrained to be below 4×10^{-18} when the

trap is well compensated to minimize RF micro-motion from stray static electric fields. The micro-motion of the trap is continuously monitored,¹¹ and; if need be, corrected by use of small bias voltages applied to either endcap and/or to two bias electrodes.

The ($^2S_{1/2} F=0$) \rightarrow ($^2D_{5/2} F=2 m_F=0$) clock transition in $^{199}\text{Hg}^+$ is first-order magnetic field insensitive at zero field and the second-order sensitivity is approximately $(-1.89 \times 10^{10} \text{ Hz T}^{-2})B^2$, where B is the magnetic field. The quadratic field shift of the clock transition due to the small ($8 \mu\text{T}$) applied quantization field is monitored during the measurement run by occasionally interleaving a frequency measurement of the first-order field sensitive ($^2S_{1/2} F=0$) \rightarrow ($^2D_{5/2} F=2 m_F=2$) component with the regular clock cycles. Slow variations of the magnetic field presently limit the uncertainty of the DC quadratic Zeeman shift to 5×10^{-18} . The maximum AC Zeeman shift caused by any asymmetry of the RF currents flowing in the trap electrodes is conservatively estimated to be less than 10^{-17} by assuming that there is no more than a 25 % imbalance of the RF currents.¹²

The electronic charge density of the $^2D_{5/2}$ state has an electric quadrupole moment that can produce an energy shift in the presence of a static electric field gradient. The magnitude and sign of the shift depend on the relative orientation of the field gradient and the applied field, which offers a route to its cancellation.¹³ Typically, the fractional frequency shift is less than 10^{-16} , but because we neither know, nor control, the ambient field gradient, the uncertainty is equally as large. However, the quadrupole shift, as well as its uncertainty, can be effectively eliminated by averaging the clock frequency for three mutually perpendicular field quantization axes.¹³ In our realization of this scheme, the orientation of the three axes and the probe light polarization were chosen to give the same scattering rate for the clock transition over the three directions of the applied magnetic field.¹¹ Changing the field direction at a regular interval (typically, every 300 s) and steering the frequency of the clock laser to resonance with the ion at each field setting are automated. The average clock frequency for the three field directions has zero quadrupole shift with a residual uncertainty of 10^{-17} . The remaining uncertainty is due to the slight nonorthogonality of the three applied fields.

The cryogenic surfaces in the Hg^+ system, adsorb all gases with the possible exception of He, so we have mounted a small cell of compressed charcoal at the bottom of the dewar that cryo-pumps the He. However, because of its limited pumping speed for He and the possibility of He leaks through, for example, the indium seals, the background He pressure could

rise to a level that could cause a significant (10^{-18}) pressure shift. An upper limit to the He partial pressure was set at 7×10^{-10} Pa by using a quadrupole mass analyzer, which is conservatively estimated to give a maximum fractional frequency shift¹² of 4×10^{-18} .

Another potential shift arises from the pulsed interrogation and detection sequence. If the clock atoms were to move synchronously with each clock cycle, the clock frequency would suffer a first-order Doppler shift with a non-zero average. This synchronized movement could have different sources, for example, the creation of photoelectric charges on ion trap electrodes due to the scattering of UV light, or, simply, motion of the trapped atom(s) with the opening or closing of mechanical shutters. The systematic shift from this effect can be substantial: a synchronized velocity of only 1) nm/s would cause a fractional frequency shift of 3×10^{-17} . The shift can be averaged away by alternately probing the optical clock resonance with collinear but counter-propagating beams. We detected no statistically significant frequency difference between the two probe directions, but an imbalance in the statistical weight of the two probe directions leads to a fractional uncertainty of 7×10^{-18} in the frequency ratio reported here.¹²

A frequency shift can be caused by the thermal loading of any acousto-optic modulator (AOM) in the clock beam path that is turned on and off, such as the stepping AOM used here to probe either side of the clock resonance. The shift appears to be a thermal effect¹⁴ that scales linearly with RF power, but diminishes as the pulse duty-cycle approaches unity. For Hg^+ the typical level of applied power during the probe "on" phase gives a maximum fractional frequency shift of 6×10^{-18} .

3. Quantum-logic Al^+ clock

Single-ion clocks based on the $^1\text{S}_0 \leftrightarrow ^3\text{P}_0$ transition of singly ionized group IIIA atoms were proposed by Dehmelt.¹⁵ Of the suggested species (B^+ , Al^+ , Ga^+ , In^+ , Tl^+), a single-ion clock based on In^+ was investigated in several experiments.^{16,17} The other group IIIA ions were considered impractical, due to the fact that their laser-cooling and state-detection atomic transitions have wavelengths in the deep UV. For the indium ion, this problem was avoided by laser-cooling and detecting fluorescence from the $^1\text{S}_0 \leftrightarrow ^3\text{P}_1$ transition. Yet, this approach is a compromise, because the scattering rate of the weakly allowed $^1\text{S}_0 \leftrightarrow ^3\text{P}_1$ transition ($\gamma = 2\pi \times 360$ kHz) limits the efficiency of laser-cooling and fluorescence detection.

Quantum-logic spectroscopy^{18,19} avoids this problem by shifting the burden of laser-cooling and fluorescence state detection to a second (logic)

ion in the same trap that has an allowed electronic transition ($\gamma \approx 10^8$ Hz). Strong Coulomb coupling between the clock and cooling ions allows for sympathetic laser cooling of the clock ion. Likewise, the coupled motion of the two ions allows efficient transfer of the clock ion's internal quantum state to the logic ion, where it can be efficiently measured.²⁰ Thus, a strongly allowed transition in the clock species is not required, which greatly expands the list of potential clock ions. The Coulomb interaction of the clock and logic ion suggests the use of a linear Paul trap to confine the ions, so that an RF nodal line exists with a simultaneous micro-motion null for both ions. In addition, the logic ion will generally produce a significant electric-field gradient on the clock ion. This favors the use of a clock transition with negligible electric-quadrupole shift.

In this article we report the results of a quantum-logic $^{27}\text{Al}^+$ clock that relies on $^9\text{Be}^+$ for sympathetic cooling and state detection. A more recent experiment combines $^{27}\text{Al}^+$ with $^{25}\text{Mg}^+$, where a quality factor for the atomic resonance of $Q = 3.5 \times 10^{14}$ was achieved.²¹ For the $\text{Al}^+ / \text{Be}^+$ clock, the systematic frequency shifts have been evaluated¹² with a fractional frequency uncertainty of 2.3×10^{-17} . Here the dominant uncertainty is due to radial micro-motion, which occurs when slowly varying electric fields in the ion trap force the ion away from the RF nodal line. These electric fields vary for two main reasons. First, electrons are sprayed through the ion trap when the ions are loaded by electron-impact ionization (typically they must be reloaded every few hours). These electrons slowly discharge during the course of the clock measurements ($\tau \approx 15$ minutes). Second, stray light from the laser beams (267 nm) that drive the $\text{Al}^+ \ ^1\text{S}_0 \leftrightarrow \ ^3\text{P}_1$ and $\ ^1\text{S}_0 \leftrightarrow \ ^3\text{P}_0$ transitions causes some parts of the ion trap to emit photoelectrons, leading to slowly varying electric fields in the ion trap. We apply real-time computer feedback to detect and eliminate the resulting micro-motion. Spot checks show that these feedback loops generally keep the magnitude of the micro-motion frequency shift below 2×10^{-17} .

The small differential polarizability between the two clock states leads to a room-temperature black-body radiation shift of $(-8 \pm 3) \times 10^{-18}$. As the ion-trap used here operates at an elevated temperature, the black-body shift for these measurements was $(-12 \pm 5) \times 10^{-18}$. The differential polarizability also couples to the electric field of the clock laser beam, whose probe period of 100 ms corresponds to an electric field amplitude in the laser beam of about $E_0 = 0.2$ V/cm. This leads to a Stark shift of much less than 1 mHz through allowed transitions and coupling to the $\ ^3\text{P}_1$ level. Because the frequency produced by the $^{27}\text{Al}^+$ clock is the average of the ($\ ^1\text{S}_0$ $F=5/2$

$m_F = \pm 5/2 \leftrightarrow ({}^3P_0 F = 5/2 m_F = \pm 5/2)$ transition frequencies near 1 Gauss magnetic field, the average can only be shifted by an imbalance in the σ_+ and σ_- polarization components in the probe beam. Such imbalances are minimized by use of π -polarized probe light that travels perpendicular to the quantization field. The effective field amplitude of this unbalanced Stark shifting field is $E_s = E_\sigma \sin \epsilon$, where $E_\sigma \leq 0.03E_0$ is the unbalanced circular polarization component of the beam, whose amplitude can be determined with a crossed polarizer, and $\epsilon \leq 0.1$ is the maximum misalignment angle of the beam. These bounds yield a maximum Stark shift of about 10^{-5} Hz. Stark shifts due to the probe beam were also tested experimentally. An increase in the probe laser power by a factor of 10000 (1 ms probe period) caused no noticeable clock shifts at the 1 Hz level, thereby reducing the uncertainty of this shift to the level of 10^{-19} in units of fractional frequency.

4. The Frequency Ratio of Al^+ to Hg^+

Figure 4(A) shows the fractional ratio instability (Allan deviation) of the two optical standards for a typical measurement run. For integration periods longer than 100 s, when the frequencies of the clocks are fully steered by the atoms, the fractional instability is $3.9 \times 10^{-15}(\tau/\text{s})^{-1/2}$. The fractional frequency instability has been improved by nearly a factor of two with respect to measurements that were made in early 2006, primarily due to decreasing the dead time and improving the duty cycle of the Hg^+ optical clock as well as incorporating a better laser reference cavity, a better cooling process and longer probe periods for the Al^+ optical clock.

Figure 4(B) shows the frequency ratio measurements of Al^+ to Hg^+ from December 2006 to November 2007. The full accuracy evaluation for the optical clocks that include corrections for the first order Doppler shifts synchronized with the probe periods has been carried out only for the last four points. The weighted average of the frequency ratio from these last four measurements is¹² $f_{\text{Al}}/f_{\text{Hg}} = 1.052871833148990438(55)$. The systematic fractional frequency uncertainties of Hg^+ (1.9×10^{-17}) and Al^+ (2.3×10^{-17}) contribute by nearly the same amount to the overall fractional uncertainty of their ratio (5.2×10^{-17}), which is dominated by a statistical uncertainty of (4.3×10^{-17}).

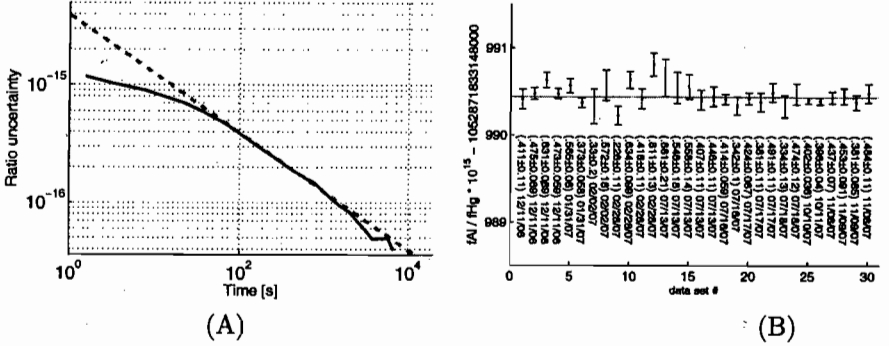


Fig. 1. (A) Allan deviation²² of a frequency ratio measurement (11 000 s total). The dashed line represents a $1/\sqrt{\tau}$ slope, beginning at 3.9×10^{-15} for 1 s. (B) History of frequency ratio measurements of the $^{199}\text{Hg}^+$ and $^{27}\text{Al}^+$ frequency standards. Error bars are statistical. Only the last four points are used in the ratio reported here,¹² as the systematic shifts for the earlier data were not as well controlled. The fractional digits of the ratio, scaled by 10^{15} , as well as the uncertainty, and the measurement date (month/day/year) are shown on the plot.

5. Test of the temporal stability of α

The fine structure constant α is the natural scaling factor for the energies involved in atomic spectroscopy. Transition frequencies from electronic (gross), fine (FS) and hyperfine (HFS) structure can be written as a function of a nonrelativistic part, which depends only on the structure involved in the transition, and a relativistic part $F_j(\alpha)$, which depends on the specific transition j that is considered. Thus the transition frequencies can be written in the following manner:^{23–25}

$$f_j(\text{el}) = R_y F_j(\alpha) \quad (1)$$

$$f_j(\text{FS}) = \alpha^2 R_y F_j(\alpha) \quad (2)$$

$$f_j(\text{HFS}) = \alpha^2 (\mu/\mu_B) R_y F_j(\alpha), \quad (3)$$

where R_y is the Rydberg constant, μ/μ_B is the ratio between the magnetic moment of the nucleus μ and the Bohr magneton μ_B .

Sensitivity to any change of R_y (temporal or otherwise) is lost in a ratio measurement, since R_y is common to all transition frequencies. The measurement of the frequency ratio of any two electronic transitions in an atom or pair of atoms returns the simplest, most direct measure of any temporal change of α . However, the measurement of the ratio of electronic transitions is not necessarily very sensitive if the precision of the measurements

is not high, and/or if the corresponding $F_j(\alpha)$ functions are not strongly disparate. $F_j(\alpha)$ contains the dependence of the specific transition involved, can be either positive or negative, and tends to be larger for transitions involving heavier atoms (where relativistic corrections play a more important role). Values of $F_j(\alpha)$ have been calculated for several atomic and molecular transitions of cosmological and laboratory interest, including^{4,26} Hg^+ and Al^+ , as well as for several HFS transitions in the microwave spectral region.⁴

Multiple measurements of the frequency ratio $r = f_{\text{Al}}/f_{\text{Hg}}$ of the optical-clock transitions of Al^+ and Hg^+ spanning about 1 year (December 2006 to November 2007) give the following result:¹²

$$\left(\frac{d}{dt}r\right)/r = (-5.3 \pm 7.9) \times 10^{-17} \text{yr}^{-1}. \quad (4)$$

From Eq. 4, the temporal variation of α can be expressed as

$$N\left(\frac{d}{dt}\alpha\right)/\alpha = \left(\frac{d}{dt}r\right)/r, \quad (5)$$

where $N = N_{\text{Al}^+} - N_{\text{Hg}^+} = 3.2$ and $N_{\text{Al}^+} \approx 0.008$. Hence, $(\frac{d}{dt}\alpha)/\alpha$ is constrained to $(-1.6 \pm 2.3) \times 10^{-17} \text{yr}^{-1}$.

This, the most stringent limit to any present-era linear change in α , is achieved primarily because of the large negative relativistic contribution for Hg^+ and the accuracy of the measurement data. The intermediate points were excluded, since the evaluation of their systematic uncertainties was incomplete. The tighter constraint made on any temporal variation of α can be used together with the 10-year record of absolute frequency measurements of the Hg^+ optical clock to tighten the coupled constraint on the possible temporal variation of the Cs magnetic moment, μ_{Cs} , to¹² $(\frac{d}{dt}\mu_{\text{Cs}})/\mu_{\text{Cs}} = (-1.9 \pm 4.0) \times 10^{-16} \text{yr}^{-1}$.

6. Stability of optical atomic clocks

There have been several studies of optical clock stability,^{27–29} but the stability limits of the newest generation of optical atomic clocks have not yet been fully explored. For these clocks the coherence times of the atoms that compose the clocks are likely to be significantly longer than the coherence times of the lasers that drive them. This is the current situation for Al^+ , where the natural linewidth of the $^1\text{S}_0 \leftrightarrow ^3\text{P}_0$ transition is 8 mHz, while the probe-laser linewidth is of order 100 mHz.³⁰ Neutral-atom-based lattice clocks³¹ are in a similar situation,³² as they are also based on doubly-forbidden $^1\text{S}_0 \leftrightarrow ^3\text{P}_0$ transitions with natural linewidths of order 10 mHz. If an isotope

without nuclear spin is chosen, such as ^{174}Yb , the natural linewidth can be made arbitrarily small.^{33,34}

While atomic resonances that are extremely narrow can be chosen for optical clocks, a fundamental noise mechanism in the probe lasers that drive these resonances has been identified, and it cannot be reduced so easily. Numata *et al.*³⁵ have found that thermomechanical noise in the length of the Fabry-Perot laser stabilization cavities leads to inevitable $1/f$ noise in the frequency of the laser local oscillator. What then is the stability of optical atomic clocks that are limited by this type of laser decoherence, and not by atomic decoherence? To address this question, some results of discrete-time numerical simulations are presented.

In this computer simulation the Ramsey method is used to probe a collection of N atoms, and dead-time is neglected, unless otherwise noted. Let t_R be the Ramsey evolution period. The discrete times of the simulations are $t_i = it_R$, where i is a non-negative integer that denotes the number of preceding measurement cycles. First, a noise signal n_i with $1/f$ spectral-density is generated³⁶ by appropriately filtering a white-noise signal in the Fourier-domain. Subsequently, the measurement-feedback cycles of the atomic clock are simulated by the iterative application of equations 6-8 on a computer.

Let c_i be the constant frequency correction applied to the clock's laser local oscillator (LO) during the time interval t_i , and let the initial correction be $c_0 = 0$. Then the clock's mean output frequency f_i during this time interval is the sum of the atomic resonance frequency ν_0 , the noise frequency n_i , and correction frequency c_i :

$$f_i = \nu_0 + c_i + n_i \quad (6)$$

This corresponds to a clock phase error of

$$\phi_i = 2\pi t_R(c_i + n_i), \quad (7)$$

which is detected through its effect on the atomic response to a Ramsey interrogation that begins at time t_i and ends at t_{i+1} . The response function is the probability $p_i = R(\phi_i)$ (see Eq. 9) that each atom is in the excited state after the Ramsey interrogation is completed. For N atoms, the total number of excitations is a binomial random variable³⁷ X_i that represents the number of successes in N tries of probability p_i . Finally, the clock's frequency correction for the next time step is calculated from the inverse atomic response function $R^{-1}(p_i)$, with a feedback gain of G :

$$c_{i+1} = c_i + \frac{G}{2\pi t_R} R^{-1}(X_i/N) \quad (8)$$

This iterative sequence is repeated many times, until the clock's long-term stability becomes apparent, i.e. the coefficient σ_0 of the stability asymptote $\sigma_y(\tau) = \sigma_0(\tau/s)^{-1/2}$ can be determined.

For the atomic response function $R(\phi)$ we take a sine wave, corresponding to the Ramsey signal from two infinitesimally short $\pi/2$ -pulses at frequency f_i separated in time by t_R , where the second pulse is phase-shifted by 90° with respect to the first:

$$R(\phi) = \frac{1}{2} (1 + \sin \phi) \quad (9)$$

$$R^{-1}(p) = \arcsin(2p - 1) \quad (10)$$

Here $R^{-1}(R(\phi)) = \phi$ for the interval $-\frac{\pi}{2} < \phi \leq \frac{\pi}{2}$. It should be noted that when the Ramsey period is maximized, the LO noise n_i may sometimes cause ϕ_i to fall outside this interval of unique invertibility. In this case, the frequency correction applied in Eq. 8 contains an "inversion error" in addition to the quantum projection noise³⁷ inherent in the random variable X_i . For this reason, atomic clocks with large atom number N and low projection noise will generally choose a somewhat shorter probe period t_R than single-ion clocks, where $N = 1$ and the projection noise is high when all other parameters are equal.

We have numerically simulated the performance of atomic clocks with different atom number N (see Fig. 2), and also shown the expected clock stability according to the well known expression³⁷

$$\sigma_y(\tau) = \frac{1}{2\pi\nu\sqrt{N\tau t_R}} \quad (11)$$

For these simulations, a laser noise floor of $\sigma_f(\tau) = 1$ Hz is assumed, which corresponds to laser frequency noise with a one-sided power-spectral-density of²² $S_f(f) = \frac{\sigma_f^2}{2f \log 2}$. The fractional frequency uncertainty $\sigma_y(\tau)$ and the frequency uncertainty $\sigma_f(\tau)$ are related by $\sigma_y(\tau) = \nu^{-1}\sigma_f(\tau)$, where ν is the clock's oscillation frequency. For the optimum Ramsey probe period we find $t_R = 0.07/\sigma_f$ and $t_R = 0.04/\sigma_f$ for $N = 1$ and $N = 10^4$ respectively. When this decoherence-limited Ramsey period is inserted into Eq. 11, we find

$$\sigma_y(\tau) = a(N) \left(\frac{\sigma_{y0}}{N\nu\tau} \right)^{1/2}, \quad (12)$$

where $a(N)$ is a numerical factor that depends very weakly on the atom number ($a(1) \approx 0.6$, $a(10^4) \approx 0.8$), and $\sigma_{y0} = \nu^{-1}\sigma_f$ is the fractional-frequency stability floor of the probe laser. Significantly, the clock stability in Eq. 12 improves as $\nu^{-1/2}$, while the improvement in Eq. 11 is ν^{-1} .

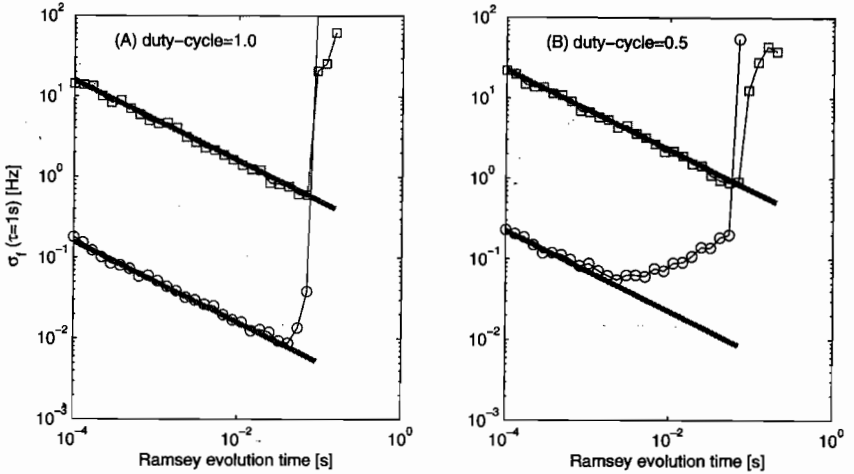


Fig. 2. Dependence of clock stability on Ramsey probe period, given a local oscillator with an Allan deviation noise floor of 1 Hz. Simulation results are shown for $N = 10^4$ atoms (\circ), and $N = 1$ atoms (\square). Thick lines show the theoretical stability given by Eq. 11, which assumes a perfect LO. The vertical axis shows the asymptotic clock stability, extrapolated to $\tau = 1$ s. Optimal probe periods are $t_R(N = 1) \approx 0.07$ s, and $t_R(N = 10^4) \approx 0.04$ s. The optimal feedback gain was found to be $G = -0.2$ for one atom, and $G = -1$ for 10^4 atoms. At long Ramsey periods, the simulated clock diverges because of LO noise. In (B) the results of the same simulation with a reduced duty-cycle of 0.5 are shown. As expected,²⁷ the loss of stability is greater for $N = 10^4$ than for $N = 1$.

This shows that entangled states³⁸ where the effective Ramsey evolution frequency is $\nu' = N\nu$ and the effective atom number is $N' = 1$ will not significantly improve the stability of the optical atomic clocks considered here, because $N'\nu' = N\nu$. The same conclusion was reached in a separate analysis.³⁹

We have performed analogous simulations for the Rabi interrogation method, and find a slight increase in the optimal probe period. However, the Ramsey method still outperforms the Rabi method, due to its sharper frequency discriminant.

7. Conclusions

We have measured the frequency ratio of two single-ion optical clocks with an accuracy of 5.2×10^{-17} . The historical record of these measurements over the course of a year shows no significant temporal variation, and indicates that the present rate of change of the fine-structure constant is no more than

a few parts in 10^{17} fractionally. The measurement uncertainty is dominated by statistical uncertainty due to clock instability, and we have explored numerically how $1/f$ frequency noise in the clock's probe laser limits the achievable stability for the Al^+ clock.

Acknowledgements

This work was supported by ONR, IARPA, and NIST. J.C.J.K. acknowledges support from the Netherlands Organisation for Scientific Research (NWO). We thank M. A. Lombardi, A. Ludlow, and D. R. Smith for their careful reading of this manuscript. This work is a contribution of NIST, and is not subject to U.S. copyright.

References

1. V. V. Flambaum, *Int. J. Mod. Phys. A* **22**, 4937 (2007).
2. S. N. Lea, *Reports on Progress in Physics* **70**, 1473 (2007).
3. T. Damour and F. Dyson, *Nuclear Physics B* **480**, 37 (1996).
4. V. A. Dzuba, V. V. Flambaum and J. K. Webb, *Phys. Rev. A* **59**, 230 (1999).
5. M. T. Murphy, J. K. Webb and V. V. Flambaum, *Mon. Not. Roy. Astron. Soc.* **345**, p. 609 (2003).
6. S. A. Levshakov, M. Centurión, P. Molaro, S. D'Odorico, D. Reimers, R. Quast and M. Pollmann, *Astronomy and Astrophysics* **449**, 879 (2006).
7. T. M. Fortier, N. Ashby, J. C. Bergquist, M. J. Delaney, S. A. Diddams, T. P. Heavner, L. Hollberg, W. M. Itano, S. R. Jefferts, K. Kim, F. Levi, L. Lorini, W. H. Oskay, T. E. Parker, J. Shirley and J. E. Stalnaker, *Physical Review Letters* **98**, p. 070801 (2007).
8. S. Blatt, A. D. Ludlow, G. K. Campbell, J. W. Thomsen, T. Zelevinsky, M. M. Boyd, J. Ye, X. Baillard, M. Fouché, R. L. Targat, A. Bruschi, P. Lemonde, M. Takamoto, F.-L. Hong, H. Katori and V. V. Flambaum, *Physical Review Letters* **100**, p. 140801 (2008).
9. W. H. Oskay, W. M. Itano and J. C. Bergquist, *Phys. Rev. Lett.* **94**, p. 163001 (2005).
10. T. Rosenband, P. O. Schmidt, D. B. Hume, W. M. Itano, T. M. Fortier, J. E. Stalnaker, K. Kim, S. A. Diddams, J. C. J. Koelemeij, J. C. Bergquist and D. J. Wineland, *Phys. Rev. Lett.* **98**, p. 220801 (2007).
11. W. H. Oskay, S. A. Diddams, E. A. Donley, T. M. Fortier, T. P. Heavner, L. Hollberg, W. M. Itano, S. R. Jefferts, M. J. Delaney, K. Kim, F. Levi, T. E. Parker and J. C. Bergquist, *Phys. Rev. Lett.* **97**, p. 020801 (2006).
12. T. Rosenband, D. B. Hume, P. O. Schmidt, C. W. Chou, A. Bruschi, L. Lorini, W. H. Oskay, R. E. Drullinger, T. M. Fortier, J. E. Stalnaker, S. A. Diddams, N. R. N. W. C. Swann, W. M. Itano, D. J. Wineland and J. C. Bergquist, *Science* **319**, p. 1808 And online supplementary materials (<http://www.sciencemag.org/cgi/content/full/1154622/DC1>) (2008).
13. W. M. Itano, *J. Res. NIST* **105**, p. 829 (2000).

14. C. Degenhardt, T. Nazarova, C. Lisdat, H. Stoehr, U. Sterr and F. Riehle, *IEEE Trans. Inst. Meas.* **54**, p. 771 (2005).
15. H. G. Dehmelt, *IEEE Trans. Inst. Meas.* **31**, p. 83 (1982).
16. J. A. Sherman, W. Trimble, S. Metz, W. Nagourney and N. Fortson, Progress on indium and barium single ion optical frequency standards (2005), arXiv.org:physics/0504013.
17. T. Liu, Y. Wang, V. Elman, A. Stejskal, Y. Zhao, J. Zhang, Z. Lu, L. Wang, R. Dumke, T. Becker and H. Walther, *Frequency Control Symposium, 2007 Joint with the 21st European Frequency and Time Forum. IEEE International*, 407 (2007).
18. D. J. Wineland, J. C. Bergquist, J. J. Bollinger, R. E. Drullinger and W. M. Itano, in *Proceedings of the 6th Symposium on Frequency Standards and Metrology*, ed. P. Gill (World Scientific, 2002).
19. P. O. Schmidt, T. Rosenband, C. Langer, W. M. Itano, J. C. Bergquist and D. J. Wineland, *Science* **309**, p. 749 (2005).
20. D. B. Hume, T. Rosenband and D. J. Wineland, *Phys. Rev. Lett.* **99**, p. 120502 (2007).
21. C.-W. Chou *et al.*, Manuscript in preparation.
22. D. B. Sullivan, D. Allan, D. A. Howe and F. L. Walls, *Characterization of Clocks and Oscillators*, Tech. Rep. 1337, NIST (1990).
23. S. G. Karshenboim, *Can. J. Phys.* **78**, 639 (2000).
24. T. M. Fortier, N. Ashby, J. C. Bergquist, M. J. Delaney, S. A. Diddams, T. P. Heavner, L. Hollberg, W. M. Itano, S. R. Jefferts, K. Kim, F. Levi, L. Lorini, W. H. Oskay, T. E. Parker, J. Shirley and J. E. Stalnaker, *Physical Review Letters* **98**, p. 070801 (2007).
25. E. Peik *et al.*, Laboratory limits on temporal variations of fundamental constants: An update, in *Proceedings of the 11th Marcel Grossmann Meeting*, (Berlin, 2006).
26. E. J. Angstmann, V. A. Dzuba and V. V. Flambaum, *Phys. Rev. A* **70**, p. 014102 (2004).
27. A. Quessada, R. P. Kovacich, I. Courtillot, A. Clairon, G. Santarelli and P. Lemonde, *Journal of Optics B: Quantum and Semiclassical Optics* **5**, S150 (2003).
28. E. Peik, T. Schneider and C. Tamm, *Journal of Physics B: Atomic, Molecular and Optical Physics* **39**, 145 (2006).
29. E. Riis and A. G. Sinclair, *Journal of Physics B: Atomic, Molecular and Optical Physics* **37**, 4719 (2004).
30. B. C. Young, F. C. Cruz, W. M. Itano and J. C. Bergquist, *Phys. Rev. Lett.* **82**, p. 3799 (1999).
31. H. Katori, M. Takamoto, V. G. Pal'chikov and V. D. Ovsiannikov, *Phys. Rev. Lett.* **91**, p. 173005 (2003).
32. M. M. Boyd, T. Zelevinsky, A. D. Ludlow, S. M. Foreman, S. Blatt, T. Ido and J. Ye, *Science* **314**, p. 1430 (2006).
33. A. V. Taichenachev, V. I. Yudin, C. W. Oates, C. W. Hoyt, Z. W. Barber and L. Hollberg, *Physical Review Letters* **96**, p. 083001 (2006).
34. Z. W. Barber, C. W. Hoyt, C. W. Oates, L. Hollberg, A. V. Taichenachev

- and V. I. Yudin, *Physical Review Letters* **96**, p. 083002 (2006).
35. K. Numata, A. Kemery and J. Camp, *Phys. Rev. Lett.* **93**, p. 250602 (2004).
 36. J. L. Lennon, *Ecography* **23**, 101 (2000).
 37. W. M. Itano, J. C. Bergquist, J. J. Bollinger, J. M. Gilligan, D. J. Heinzen, F. L. Moore, M. G. Raizen and D. J. Wineland, *Phys. Rev. A* **47**, p. 3554 (1993).
 38. J. J. . Bollinger, W. M. Itano, D. J. Wineland and D. J. Heinzen, *Phys. Rev. A* **54**, R4649 (1996).
 39. D. J. Wineland, C. Monroe, W. M. Itano, D. Leibfried, B. E. King and D. M. Meekhof, *J. Res. NIST* **103**, p. 259 (1998).